BIOCHEMISTRY
including biophysical chemistry & molecular biology
Article

Biochemistry **2009,** *48,* 11745–11754 11745
DOI: 10.1021/bi901387k

Studies of the Expression of Human Poly(ADP-ribose) Polymerase-1 in *Saccharomyces cerevisiae* and Identification of PARP-1 Substrates by Yeast Proteome Microarray Screening[†]

Zhihua Tao,[‡] Peng Gao,[‡] and Hung-wen Liu*[,‡,§]

[§]*Division of Medicinal Chemistry, College of Pharmacy, Department of Chemistry and Biochemistry,* [‡]*Institute for Cellular and Molecular Biology, University of Texas at Austin, Austin, Texas 78712*

Received August 10, 2009; Revised Manuscript Received October 29, 2009

ABSTRACT: Poly(ADP-ribosyl)ation of various nuclear proteins catalyzed by a family of NAD^+-dependent enzymes, poly(ADP-ribose) polymerases (PARPs), is an important posttranslational modification reaction. PARP activity has been demonstrated in all types of eukaryotic cells with the exception of yeast, in which the expression of human PARP-1 was shown to lead to retarded cell growth. We investigated the yeast growth inhibition caused by human PARP-1 expression in *Saccharomyces cerevisiae*. Flow cytometry analysis reveals that PARP-1-expressing yeast cells accumulate in the G_2/M stage of the cell cycle. Confocal microscopy analysis shows that human PARP-1 is distributed throughout the nucleus of yeast cells but is enriched in the nucleolus. Utilizing yeast proteome microarray screening, we identified 33 putative PARP-1 substrates, six of which are known to be involved in ribosome biogenesis. The poly(ADP-ribosyl)ation of three of these yeast proteins, together with two human homologues, was confirmed by an *in vitro* PARP-1 assay. Finally, a polysome profile analysis using sucrose gradient ultracentrifugation demonstrated that the ribosome levels in yeast cells expressing PARP-1 are lower than those in control yeast cells. Overall, our data suggest that human PARP-1 may affect ribosome biogenesis by modifying certain nucleolar proteins in yeast. The artificial PARP-1 pathway in yeast may be used as a simple platform to identify substrates and verify function of this important enzyme.

Poly(ADP-ribose) polymerase-1 (PARP-1),[1] an abundant nuclear protein with DNA damage sensing activity, has been implicated in cell cycle regulation, DNA repair, transcription, and cell death (*1*−*3*). The numerous functions of PARP-1 in various cellular processes underlie its diverse roles in many physiological and pathological pathways including maintenance of genomic integrity, carcinogenesis, aging, inflammation, and neurodegerative disorders (*2*). Upon activation by damaged DNA, PARP-1 catalyzes the synthesis of poly(ADP-ribose) polymers (PAR) onto both target proteins and itself using NAD^+ as the source of ADP-ribose. Under normal physiological conditions, basal PARP-1 activity is required for the regulation of gene expression during development and in response to specific cellular and environmental signals (*4*, *5*). PARP-1 activation under low levels of DNA breaks caused by mild genotoxic stress stimulates the base excision repair machinery to repair DNA and to facilitate cell survival. In contrast, overactivation of PARP-1 by excessive DNA damage caused by severe oxidative stress will deplete cellular NAD^+ and ATP, which eventually leads to necrotic cell death. Various molecular and genetic approaches including *parp-1* knockout (*6*, *7*), overexpression of PARP-1 (*8*), introduction of PARP-1 antisense RNA (*9*), and PARP-1 inhibitors (*10*) have contributed to our understanding of the biological roles of PARP-1. However, the exact molecular functions that PARP-1 fulfils in many of these processes have not yet been determined.

Elucidation of the functions of PARP-1 requires a clarification of PARP-1 substrate proteins and interaction partners. More than 30 PARP-1 substrates including histones, HMG proteins, topoisomerases I and II, DNA and RNA polymerases, p53, transcription factors YY1 and NF-κB, and nucleolar proteins B23 (nucleophosmin) and C23 (nucleolin) have been identified *in vivo* and *in vitro* by various approaches such as copurification, coimmunoprecipitation, cross-linking, and yeast two-hybrid screening (*1*). These substrates are almost exclusively involved in the metabolism of nucleic acids and the maintenance of chromatin architecture. Although the detailed physiological consequences of protein poly(ADP-ribosyl)ation are unknown, it is conceivable that the polyanionic nature of PAR could inhibit the interaction of modified acceptor proteins with other negatively charged molecules such as DNA or that the addition of PAR to the active site of an enzyme may change its enzymatic properties (*1*).

[†]This work was supported in part by grants from TI-3D and the Welch Foundation (H-F-0032 and F-1511).

*To whom correspondence should be addressed. Phone: (512) 232-7811. Fax: (512) 471-2746. E-mail: h.w.liu@mail.utexas.edu.

[1]Abbreviations: BSA, bovine serum albumin; cfu, colony-forming units; CT-DNA, calf thymus DNA; DTT, dithiothreitol; GFP, green fluorescent protein; HEPES, 4-(2-hydroxyethyl)-1-piperazineethanesulfonic acid; HPLC, high-performance liquid chromatography; HRP, horseradish peroxidase; IgG, immunoglobulin G; IPTG, isopropyl α-D-thiogalactopyranoside; LB, Luria−Bertani; NAD^+, nicotinamide adenine dinucleotide (oxidized form); NLS, nuclear localization signal; Ni-NTA, nickel nitrilotriacetic acid; PAGE, polyacrylamide gel electrophoresis; PAR, poly(ADP-ribose); PARG, poly(ADP-ribose) glycohydrolase; PARP-1, poly(ADP-ribose) polymerase-1; PBS, phosphate-buffered saline; PBST, PBS containing 0.1% (v/v) Tween 20; PMSF, phenylmethanesulfonyl fluoride; SC, synthetic complete media; SDS, sodium dodecyl sulfate; TBS, Tris-buffered saline; TBST, TBS containing 0.1% (v/v) Tween 20.

Published on Web 10/30/2009

PARP-1 is the first characterized PARP. To date, 17 members of the PARP family have been identified based on their amino acid sequence similarity to the catalytic domain of PARP-1 (*11*). The presence of multiple PARPs in mammals further complicates the analysis of each PARP function *in vivo*. Although each PARP has unique characteristic features, some of these proteins display functional redundancy. For example, some PARPs colocalize and heterodimerize with each other, while others share the same substrate proteins (*12*−*14*). Thus, how to correlate a phenotype to the function of one specific or several PARP enzymes has been a challenging task.

Interestingly, PARP activity is absent in yeast despite the fact that it is found in organisms ranging from archaebacteria to mammals. Thus, it has been suggested that the biological roles of PARP enzymes may be conveniently probed by expressing each of the targeted PARP enzymes in yeast (*15*−*17*), organisms that share many physiological features with higher eukaryotes. Further support comes from early work showing that expression of PARP-1 in yeast led to inhibition of cell division and to morphological changes reminiscent of those observed in yeast cell cycle mutants (*15*). Moreover, this effect could be attenuated by the addition of established PARP inhibitors or the coexpression of poly(ADP-ribose) glycohydrolase (PARG), an enzyme that degrades the PAR polymers synthesized by PARP (*15*, *18*). However, the mechanism of such inhibition has not been investigated in detail.

Encouraged by the early observations and the successful use of yeast cells to identify genes involved in mammalian apoptosis (*19*), we decided to explore the feasibility of using yeast as a model system to study and understand the complex physiological processes mediated by PARP catalysis. In this report, we first investigated the underlying mechanism of yeast growth inhibition by expressing human PARP-1 in *Saccharomyces cerevisiae*. Our data showed that expression of human PARP-1 in yeast delays the cell cycle at the G_2/M stage. The heterologously expressed human PARP-1 was found to be localized in the nucleus and concentrated in the nucleolus of yeast. Consistent with this observation, several proteins involved in ribosome synthesis are identified as protein substrates for PARP-1 by yeast proteome microarray screening. Several of the yeast proteins identified in the microarray screening along with their human homologues are found to undergo poly(ADP-ribosyl)ation using *in vitro* PARP-1 activity assays. To the best of our knowledge, this is the first time that PARP-1 substrates are identified by high-throughput screening. Polysome profile analysis also revealed that ribosome levels are decreased in yeast cells expressing PARP-1, suggesting a potential role for PARP-1 in regulating ribosome production. The fact that several human proteins involved in ribosome biogenesis are also substrates of PARP-1 implicates analogous roles for PARP-1 in humans. Taken together, our results demonstrate that yeast may provide a convenient platform to identify and to study protein substrates for human PARP enzymes.

MATERIALS AND METHODS

Plasmids. The human *parp-1* gene was amplified from the cDNA library of HeLa cells by polymerase chain reaction (PCR) and cloned into pET-28b (Novagen, Madison, WI) at the *Nde*I and *Xho*I sites. To subclone the PARP-1 gene into the yeast shuttle vector pYES2 (Invitrogen, Carlsbad, CA), the *parp-1* gene was first PCR-amplified using PARP-1/pET-28b as the template and 5′-CGCGGAGCTCCATATGGCGGAGTCTTC-3′ (forward) along with the T7 terminator (reverse) as primers, digested with *Sac*I and *Xho*I, and then ligated into the same restriction sites of pYES2. The Kozak translation initiation sequence, ANNATGG, was introduced at the beginning of the *parp-1* gene by site-directed mutagenesis using 5′-GCTTGGTACCGAGCTCAATATGG-CGGAGTCTTCG-3′ and 5′-CGAAGACTCCGCCATATT-GAGCTCGGTACCAAGC-3′ (with the mutated codon underlined) as the forward and reverse primer, respectively. The PARP-1 E988A mutant was obtained by mutagenesis using PARP-1/pET-28b as the template and 5′-CTATATAACGCGTA-CATTGTC-3′ (forward) and 5′-GACAATGTACGCGTTATA-TAG-3′ (reverse) as primers (with the mutated codon underlined). The resulting PARP-1 E988A/pET-28b was cut by *Asc*I and *Xho*I, and the excised fragment was used to replace the sequence between *Asc*I and *Xho*I in PARP-1/pYES2, thus producing PARP-1 E988A/pYES2.

The PARP-1-GFP/pYES2 plasmid, containing the human *parp-1* gene fused in-frame to the 5′-end of the gene encoding green fluorescent protein, was constructed according to a method reported by Geiser et al. (*20*). Briefly, the GFP gene was amplified from pGFPuv (Clontech, Palo Alto, CA) by primers 5′-CAATT TTAAGACCTCCCTGTGGCGGGTACCGGTAGAAAAA-ATGAG-3′ (forward) and 5′-GCGGCCCTCTAGATGCAT-GCTCGAGTTATTTGTAGAGCTCATCCATGCC-3′ (reverse). The resulting PCR fragment, carrying the GFP-encoding sequence flanked on its 5′- and 3′-ends by sequences homologous to the 3′-end of *parp-1* gene and the pYES2 vector, respectively, was annealed to the methylated template pYES2-PARP-1. After elongation with *pfu* Turbo DNA polymerase (Stratagene, La Jolla, CA) and digestion of the template DNA with *Dpn*I, the new PARP-1-GFP/pYES2 plasmid was transformed into *Escherichia coli* strain DH5 (Novagen) for plasmid amplification. The plasmid pAJ1076, carrying the gene sequence of DsRed-Nop1, was a generous gift from Dr. Arlen W. Johnson (Institute of Cellular and Molecular Biology, University of Texas at Austin).

The cDNAs encoding yeast NOB1, HAS1, and LHP1 (kindly provided by Dr. Michael Snyder, Department of Molecular Biophysics and Biochemistry, Yale University) were amplified by PCR and subcloned into pET-28b at the *Sac*I and *Xho*I sites. The recombinant proteins were expressed as N-terminal His_6-tagged proteins under the control of a T7 promoter. The cDNA for human La protein was cloned from the HeLa cDNA library by the primers 5′-CGCGCATATGCCTCGAAAAAG-3′ (forward) and 5′-CCGGCTCGAGTCACTTTCCCAAA-GTC-3′ (reverse). The PCR product was digested by *Nde*I and *Xho*I and ligated into the corresponding restriction sites in pET-28b. Human DDX47 was amplified from a HeLa cDNA library with the primers 5′-GGGAATTCCATATGGCGGCACCC-GAGGAAC-3′ and 5′-GTATTTGAATGCGGCCGCTTAAC-GGCCTTTCCGCTTC-3′ and cloned between the *Nde*I and *Not*I sites of pET-28b.

Strain and Medium. The *S. cerevisiae* strain used in this study was W303-1a (*MAT*a, *can1*−*100*, *leu2*−*3*, *leu2*−*112*, *his3*−*11*, *trp1*−*1*, *ura3*−*1*, *ade2*−*1*). Cells transformed with pYES2 or PARP-1/pYES2 were maintained in SC minimal media with uracil as the selection marker (SC-U). The gene expression was repressed in the presence of 2% glucose (SC-U-Glu) and was induced in the presence of 2% galactose (SC-U-Gal). Cells transformed with PARP-1-GFP/pYES2 and pAJ1076 were maintained in SC minimal media plates lacking both uracil and leucine (SC-U-L).

Growth Curve Analysis. Yeast cultures were grown at 30 °C in SC-U-Glu medium to the saturation stage, washed twice by induction media (SC-U-Gal), and diluted 1:50 into the same induction media. Cell growth was measured by monitoring the turbidity of the cell cultures at 600 nm with a spectrophotometer. Absorbance readings, taken every 2 h, were plotted against induction time, and the data were used for calculating the doubling time. For inhibitor treatment, either 3 mM 3-aminobenzamide (Sigma, St. Louis, MO) or 100 μM 6(5*H*)-phenanthridinone (Alexis, San Diego, CA) was added to the medium at the same time of induction. To determine the viability of *S. cerevisiae* by counting colony-forming units (cfu), the yeast cells were grown in SC-U-Gal to an OD_{600} of 0.6 and 100 μL of serially diluted samples was surface-plated in duplicate on SC-U-Gal plates. Plates were cultured at 30 °C for 4 days, and the number of colonies was counted. Dilution factors were multiplied back to obtain cfu/mL of culture.

Western Blotting Analysis of PAR in Yeast. The cell lysates from the recombinant yeast strains were extracted using YER reagent (Invitrogen) following the manufacturer's protocol. Cell extracts were separated using 12% SDS−PAGE gel up to the staining step. The proteins were then electrophoretically transferred to a nitrocellulose membrane (100 V × 1 h, 4 °C) with cold running buffer containing 25 mM Tris base, 192 mM glycine, and 20% methanol at pH 8.3. The membrane was blocked with 5% (w/v) nonfat dry milk in TBST (20 mM Tris-HCl, pH 7.5, 150 mM NaCl, 0.1% (v/v) Tween 20) at room temperature for 1 h. The membrane was then incubated with mouse anti-PAR polyclonal antibody (Trevigen, Gaithersburg, MD) for 1 h, washed three times with TBST buffer, and incubated with goat anti-mouse IgG horseradish peroxidase (HRP) conjugate (Pierce, Rockford, IL) for 1 h. After three washes with TBST buffer, the bound antibody was visualized by the Pierce chemiluminescence detection system according to the manufacturer's instruction.

Flow Cytometry Analysis. For cell cycle analysis, yeast cultures were grown in SC-U-Glu to saturation, washed twice by SC-U-Gal media, and diluted 50-fold with 10 mL of SC-U-Gal media. After 16 h of galactose induction, approximately 10^7 cells were collected by centrifugation (2500*g*, 0.5 min). Cells were washed with 1 mL of cold PBS (1.5 mM KH_2PO_4, 8 mM Na_2HPO_4, pH 7.4, 2.7 mM KCl, 137 mM NaCl) and pelleted by centrifugation (2500*g*, 0.5 min). Cells were resuspended in 1 mL of 70% cold ethanol and allowed to incubate at 4 °C with shaking for 24 h. An aliquot of 300 μL of the ethanol-fixed samples was pelleted by centrifugation and washed with 1 mL of PBS. Cells were again pelleted by centrifugation, and the supernatant from the wash was decanted. Cells were resuspended in 1 mL of PBS containing 1 mg/mL RNase A and incubated at 37 °C for 2 h, after which 5 μL of 1 mg/mL propidium iodide (MP Biomedicals, Solon, OH) was added, and cells were incubated on ice for 30 min. From each sample, 40000 cells were scanned with a Beckman Coulter Cytomics FC 500 flow cytometer.

Fluorescence Microscopy. Cells expressing PARP-1-GFP alone or with DsRed-Nop1 were grown in glucose-containing medium until saturation. Cells were diluted to OD_{600} 0.4 in galactose-containing medium and allowed to grow for an additional 20 h. To visualize PARP-1-GFP and DsRed-Nop1 in living cells, 400 μL of yeast culture was collected by centrifugation, washed with water, and resuspended in 400 μL of water. The DNA was stained by incubating the cells with 4 μM Hoescht 33342 at room temperature for 30 min. Twenty microliter aliquots of cells were then spotted on glass slides, and the coverslips were sealed with nail polish. Confocal imaging was performed using a Leica SP2 AOBS microscope with a 63× oil-immersion lens. For multitrack imaging, GFP was excited with 488 nm light from an argon line, and the emission was collected using a 495−527 nm band-pass filter. DsRed was excited with 543 nm light from a HeNe line, and the emission was collected using a 583−650 nm band-pass filter. Hoescht 33342 was excited with UV light, and the emission was collected using a 418−466 nm band-pass filter. Further processing of images was performed using Adobe Photoshop 7.0 (Adobe Systems, San Jose, CA).

Proteome Microarray. The biotinylated NAD^+ was prepared according to a literature procedure (*21*) using 8-[(6-aminohexyl)amino]NAD (Sigma) and EZ-link NHS-LC-biotin (Pierce). The ProtoArray yeast proteome microarray nc v1.0 (Invitrogen) was used to detect poly(ADP-ribosyl)ation of yeast proteins by PARP-1. The proteome chip was first blocked with 25 mL of PBST by incubating at 4 °C for 1 h with gentle shaking. After decanting the PBST blocking buffer, the chip was probed with 1 mL of PARP-1 reaction mixture containing 4 mM $MgCl_2$, 0.2 mM DTT, 10 μg/mL activated calf-thymus DNA (CT-DNA), 20 μM NAD^+, and 20 μM biotinylated NAD^+ in 50 mM Tris-HCl (pH 8.0). The poly(ADP-ribosyl)ation reaction was initiated by the addition of 1 μM purified PARP-1. The array was subsequently incubated at 25 °C for 30 min. Following incubation, the array was then washed three times using 25 mL of high-salt wash buffer (PBS with 1 M NaCl) to disrupt non-covalent interactions. The array was then incubated with Alexa Fluor 647 streptavidin and then read with an Axon GenePix 4000 scanner. Data were acquired with GenePix Pro and further analyzed using Protoarray Prospector software, which collects all the signals from the proteins on the array and calculates the mean value and standard deviation. The *Z*-score for an individual data point in a population reflects its deviation from the mean in units of standard deviations. The yeast proteins that had a *Z*-score greater than 3 were considered as positive substrates for PARP-1. Human homologues of the yeast proteins were identified using the BLASTP search provided by the National Center of Biological Information (www.ncbi.nlm.nih.gov).

Protein Purification. The plasmids expressing His_6-tagged human PARP-1, NOB1, HAS1, LHP1, human La, and DDX47 were transformed into *E. coli* Rosseta 2BL21(DE3), and the transformants were selected by plating against kanamycin (50 μg/mL) and chloramphenicol (35 μg/mL). Typically, protein overexpression was carried out by inoculating 1 L of LB medium containing 50 μg/mL kanamycin with 1 mL of saturated overnight culture. Bacteria were grown in LB broth at 37 °C until the OD_{600} reached 0.6, at which point the cells were induced with 0.2 mM IPTG and subsequently cultured at 18 °C for 24 h. Cells were harvested by centrifugation (7000*g*, 10 min), and the resulting pellets were stored at −80 °C until lysis.

Thawed cells were resuspended in lysis buffer (20 mM HEPES, pH 7.5, 300 mM NaCl, 10 mM imidazole, 10% glycerol) at 40 mL of buffer/L of culture. Cell suspensions were sonicated on ice using six 20 s bursts with 1 min cooling periods. Cell debris was removed by centrifugation (20000*g*, 30 min), and the supernatant was incubated with 5 mL of Ni-NTA agarose resin (Qiagen, Valencia, CA) on a rotator at 4 °C for 1 h. Lysate and resin were then loaded onto a column, which was drained and then washed with 50 mL of lysis buffer, followed by 10 mL of wash buffer (20 mM HEPES, pH 7.5, 1 M NaCl, 10 mM imidazole, 10% glycerol). The bound, His_6-tagged protein was eluted from the column with elution buffer containing 20 mM HEPES,

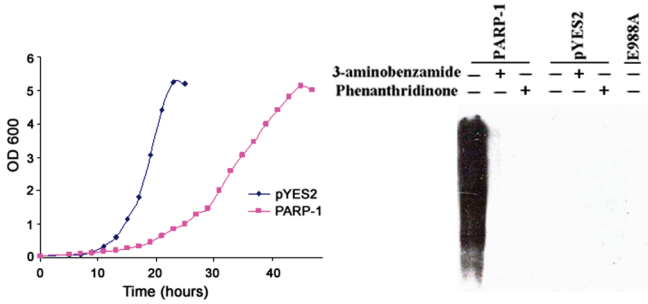

strains	no inhibitor treatment	3-aminobenzamide	phenanthridinone
pYES2	2.8	2.9	3.0
PARP-1	7.6	3.0	3.0
E988A	2.8	ND	ND

A B C

FIGURE 1: Expression of human PARP-1 in yeast causes growth delay. (A) Growth curves for pYES2 control yeast cells and PARP-1-expressing yeast cells. Cultures were grown in SC-U-Glu media at 30 °C until stationary phase and then diluted 50-fold in SC-U-Gal media. The growth was monitored by measuring the OD_{600}. (B) The PAR produced in yeast transformants was detected by Western blotting analysis with anti-PAR antibody. PAR was produced in PARP-1-expressing cells but not in pYES2 control cells or E988A-expressing cells. PARP-1 inhibitors effectively inhibit PAR formation in yeast cells. (C) The doubling time (in hours) of yeast transformants was determined during logarithmic growth. The doubling times for PARP-1-expressing cells, pYES2 control cells, and E988A-expressing cells are 7.6, 2.8, and 2.8 h, respectively. PARP-1 inhibitors can rescue the growth delay of PARP-1-expressing cells. ND, not determined.

pH 7.5, 300 mM NaCl, 250 mM imidazole, and 10% glycerol. The desired protein fractions were pooled and dialyzed against 3 × 1 L of lysis buffer. The purified protein was aliquoted, flash-frozen, and stored at −80 °C until use.

Poly(ADP-ribosyl)ation Assay. For the poly(ADP-ribosyl)ation dot blot assay, 2−4 μg of PARP-1 substrates (NOB1, HAS1, and LHP1) were spotted onto a nitrocellulose membrane and blocked with 10 mg/mL BSA for 2 h. PARP-1, histones, and BSA were also spotted on the membrane to serve as positive and negative controls, respectively. After being washed with PBS, the membrane was incubated with 5 mL of reaction buffer (100 mM Tris-HCl, pH 7.0, 10 mM $MgCl_2$) containing 10 μg/mL activated CT-DNA and 0.1 μM PARP-1 (or without PARP-1 as control). Reactions were initiated by the addition of 16 μM NAD^+ containing 1 μCi of [^{32}P]NAD^+. Reactions were allowed to proceed for 5 min at room temperature and arrested by decanting the reaction mixture from the membrane. The membrane was then washed three times using high salt buffer (100 mM Tris-HCl, pH 7.0, 1 M NaCl), allowed to air-dry, wrapped in plastic film, and exposed to a phosphorimaging screen for 24 h. The exposed screen was read by PhosphorImage using the Scanner Control program (Molecular Dynamics, Sunnyvale, CA).

Poly(ADP-ribosyl)ation assays were also performed in 20 μL reaction mixtures containing 0.1 μM PARP-1 (or without PARP-1 as a negative control), 1 μM substrate proteins, 10 μg/mL activated CT-DNA, 1 μM NAD^+, 0.1 μCi of [^{32}P]NAD^+, 100 mM Tris-HCl, pH 7.0, and 10 mM $MgCl_2$ for 10 min at room temperature. Reactions were quenched by adding an equal volume of 2× SDS loading buffer. Reaction mixtures were then resolved using a 12% SDS−PAGE gel. Following electrophoresis, the gel was dried on filter paper using a vacuum gel dryer (Bio-Rad, Hercules, CA) at 60 °C for 30 min. The dried gel was subjected to phosphorimaging analysis using the same PhosphorImage and software described above.

Polysome Analysis. Polysome preparation was carried out according to the procedure of West et al. (*22*) with some modifications. Briefly, a saturated, overnight culture of yeast cells expressing PARP-1 or control cells, grown at 30 °C in SC-U-Glu media, was diluted 80-fold with 250 mL of SC-U-Gal induction media. The culture was incubated at 30 °C until the OD_{600} reached 0.5. To the culture was added 150 μg/mL cycloheximide, and the culture was immediately incubated in ice water for 20 min. All of the following steps were carried out at 4 °C.

Cells were collected by centrifugation (4000*g*, 10 min). The cell pellet was washed with 12 mL of ice-cold breaking buffer (10 mM Tris-HCl, pH 7.4, 100 mM NaCl, 30 mM $MgCl_2$, 14 mM -mercaptoethanol, 1 mM PMSF, 0.2 mM EDTA, 1 μg/mL each of leupeptins and pepstatin A, 200 μg/mL cycloheximide, and 200 μg/mL heparin). Cells were pelleted again by centrifugation (4000*g*, 5 min) and then resuspended into 800 μL of the same breaking buffer containing protease inhibitor cocktail (Roche, Palo Alto, CA). Acid-washed glass beads (400−625 μm; Sigma) were added to the cell suspension to approximately one-fourth of the total volume. The glass bead−cell mixture was vortexed vigorously with a vortex mixer (ten times for 20 s with 30 s intervals on ice) to break the cell walls. Insoluble material was removed by two sequential centrifugation steps (5000*g*, 5 min; 12000*g*, 10 min). Ten OD_{260} units of supernatant was loaded onto a 36 mL linear sucrose gradient (7−42%) and was subjected to ultracentrifugation for 4 h at 141000*g* in a Beckman SW 28 rotor at 4 °C. Sucrose gradient fractions were analyzed by UV absorbance at 254 nm.

RESULTS

Effects of PARP-1 Expression on Yeast Cell Growth, Cell Viability, and Cell Cycle Progression. Human PARP-1 has been expressed in the *S. cerevisiae* budding yeast W303 haploid strain under the inducible promoter *GAL1*. The empty expression vector pYES2 was also transformed into W303 as a control. Yeast growth, as determined by measuring the turbidity of the culture at 600 nm, was inhibited by the heterologous expression of PARP-1 (Figure 1A). In galactose-containing SC-U medium, the doubling times for the pYES2 control and PARP-1-expressing cells at log phase are 2.8 and 7.6 h, respectively (Figure 1C). Both strains exhibit the same growth rate when glucose was used as the carbon source (data not shown). Our data also show that PARP-1 is active in yeast even without treatment by DNA damaging reagents. The Western blotting analysis of total yeast extracts with a PAR polyclonal antibody shows smears and undifferentiated bands indicating the presence of poly(ADP-ribosyl)ated proteins with different molecular masses (Figure 1B). It is apparent that poly(ADP-ribosyl)ation in yeast is responsible for the growth inhibition, since yeast expressing E988A, a PARP-1 mutant lacking poly(ADP-ribosyl)ation activity, grows as well as the wild-type strain. Also, PARP-1

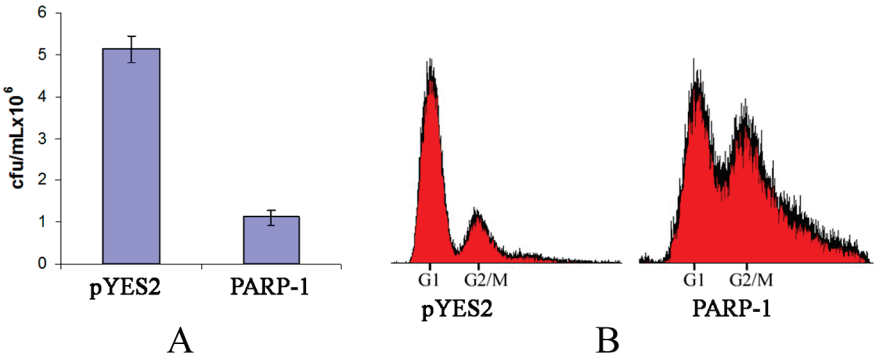

FIGURE 2: Effects of PARP-1 expression on yeast cell viability and cell cycle progression. (A) Viability of pYES2 control cells and PARP-1-expressing cells assayed by plate count experiments. The number of viable cells in each sample was estimated by their ability to form colonies on solid SC-U-Gal media over 4 days at 30 °C. At an OD_{600} of 0.6, the viable counts for pYES2 control cells were 5.13×10^6/mL, while that of PARP-1-expressing cells decreased to 1.11×10^6/mL. The error bar represents standard derivation. (B) Flow cytometric analysis of pYES2 control cells and PARP-1-expressing yeast cells. PARP-1-expressing yeast cells exhibited a larger peak corresponding to G_2/M nuclei than the pYES2 control cells.

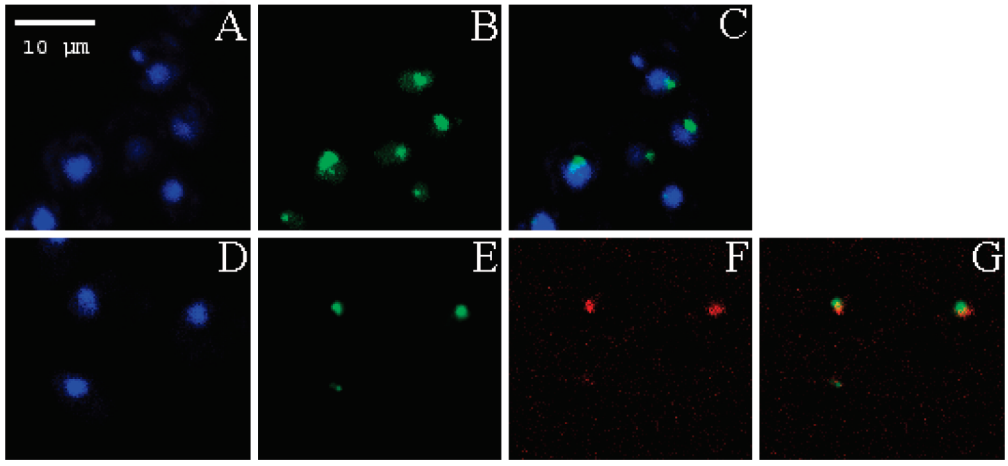

FIGURE 3: Heterologously expressed human PARP-1 is localized in the yeast nucleus and is concentrated in the nucleolus. Cells harboring different plasmids were induced in SC-U-Gal or SC-U-L-Gal media for 12 h. GFP (green), DsRed (red), and Hoechst (blue) fluorescence signals were detected by confocal microscopy. (A−C) PARP-1-GFP localization. (A) Hoechst; (B) PARP-1-GFP; (C) merged images of Hoechst and PARP-1-GFP signals. (D−G) PARP-1-GFP/DsRed-Nop1 colocalization. (D) Hoechst; (E) PARP-1-GFP; (F) DsRed-Nop1; (G) merged images of PARP-1-GFP and DsRed-Nop1 signals.

inhibitors 3-aminobenzamide (3 mM) and 6(5*H*)-phenanthridinone (100 μM) effectively inhibit PARP-1 activity in cells, rescuing the growth delay (Figure 1B,C). These results are in agreement with those previously reported (*18*).

The growth curve analysis is based on the turbidity of the culture, which cannot distinguish between living and dead cells. Thus, more experiments were carried out to assess if PARP-1 expression causes the necrotic or apoptotic death of yeast cells. The majority of both control yeast cells and PARP-1-expressing cells in SC-U-Gal medium stained negative in trypan blue exclusion assays, indicating that the cells are still alive following PARP-1 expression (data not shown). In addition, negative staining is also observed in the annexin V/propidium iodide assay. This result indicates the absence of phosphatidylserine at the cell membrane or reduced membrane integrity, which are early indicators of cellular apoptosis (data not shown). Although PARP-1 cells remain alive, most of them fail to replicate to form colonies on SC-U-Gal plates, as demonstrated by the plate count assay (Figure 2A). At an OD_{600} of 0.6, the viable counts for pYES2 control cells were 5.13×10^6/mL, while that of PARP-1-expressing cells decreased to 1.11×10^6/mL, indicating a defect in cell division caused by PARP-1 expression (Figure 2A). Flow cytometry analysis revealed that asynchronous PARP-1-expressing yeast cells have a marked accumulation in the G_2/M phase (Figure 2B). Thus, the observed slow growth rate of PARP-1 cells is most likely due to cell cycle arrest.

Expressed Human PARP-1 Is Localized in the Yeast Nuclei and Is Concentrated in the Nucleoli. Previously, heterologously expressed human PARP-1 was found to localize in the yeast nucleus by indirect immunofluorescence staining (*15*). To verify that the nuclear localization signal within the PARP-1 sequence indeed directs the expressed PARP-1 protein to the nucleus in the yeast strain used in this study, we constructed PARP-1-GFP/pYES2. This construct was designed to determine directly the localization of the fusion proteins in live yeast cells. This design minimizes the effects of nonspecificity often seen with immunostaining and cell fixation, and the result likely represents the heterologous PARP-1 localization in yeast under physiological conditions. As shown in Figure 3A−C, the green fluorescence signal of PARP-1-GFP is distributed throughout the entire nucleus in yeast but is highly concentrated in a crescentic area close to the nuclear periphery, which resembles the typical nucleolar staining pattern. To confirm the identity of this small area, DsRed-Nop1, where DsRed is fused with the nucleolar protein Nop1 (the yeast homologue of fibrillarin), was used as a nucleolar marker and was coexpressed with PARP-1-GFP in

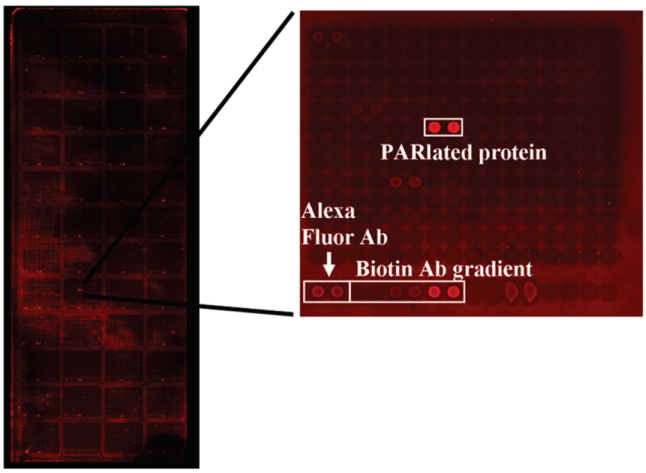

FIGURE 4: Image of poly(ADP-ribosyl)ated proteins on the yeast proteome microarray. (A) Array image. (B) One of the 48 subarrays shown in detail. Alexa Fluor 647 antibody and various amounts of a biotinylated anti-mouse antibody were printed on the microarray to serve as positive controls. A poly(ADP-ribosyl)ated yeast protein (printed on the array in duplicate) is boxed.

yeast. As expected, the DsRed-Nop1, detected by the DsRed fluorescence, exhibits a typical crescent staining of the nucleolus, which does not overlap with the DNA staining (Figure 3E). Merging the GFP and DsRed images clearly shows the colocalization of PARP-1-GFP and DsRed-Nop1 (Figure 3G). Interestingly, the signals from PARP-1-GFP and DsRed-Nop1 are always only partially overlapped, which suggests that although PARP-1 is enriched in the yeast nucleolus, its subnucleolar compartmentalization may be somewhat different from that of Nop1.

Yeast Proteome Microarray Screening Identifies PARP-1 in Vitro Substrates. The existence of PAR acceptors in yeast, indicated by our Western blotting analysis and studies conducted by others (*16*), prompted us to further investigate the identity of these proteins. Toward this goal, we successfully immunoprecipitated some PARlated proteins from yeast extracts using anti-PAR antibody (data not shown). However, the heterogeneity of the PAR attached on the acceptor proteins, namely, the different length of each polymer chain and the multitude of branching points within each polymer chain, makes it difficult to analyze these acceptor proteins by mass spectrometry. Moreover, the sequence specificity of poly(ADP-ribosyl)ation is poorly understood, which diminishes the power of genome-wide bioinformatics screens to identify putative PARP-1 substrates. In contrast, the readily available and more affordable yeast proteome microarray, which includes 80% of the total proteins produced by *S. cerevisiae*, provides a convenient and high-throughput screening method for our intended study. We have utilized the yeast proteome microarray to screen for PARP-1 substrates *in vitro*.

In trial assays, human histones (as a positive control) and BSA (as a negative control) were first blotted onto the nitrocellulose-membrane-coated glass slides to test the assay conditions before using the commercial yeast proteome microarray purchased from Invitrogen. The optimal transmodification conditions for PARP-1 were established by varying concentrations of PARP-1, biotinylated NAD^+, and CT-DNA. These optimized conditions were then applied in the proteome microarray screening. The yeast microarray chips were first incubated with the PARP-1 reaction mixture containing biotinylated NAD^+ as described in Materials and Methods. The PARlated yeast proteins on the array were detected by incubating the array with Alexa Flour 647 streptavidin. Figure 4 shows the array image and the image of a subarray as an example. Using the Protoarray Prospector software, 33 yeast proteins with *Z*-scores higher than 3 were identified as potential PARP-1 substrates (Table 1). Among these 33 proteins, 22 are nuclear proteins, and 6 of them are localized in nucleoli. The 6 nucleolar proteins have been reported to be involved in ribosome biogenesis and RNA processing. Most of these PARlated yeast proteins are nucleic acid binding proteins. The mechanisms and the effects of poly(ARP-ribosyl)ation on these proteins are discussed in more detail below.

In view of the PARP-1 cellular localization, the nuclear and nucleolar substrates identified by proteome microarray screening might be more physiologically relevant. We are particularly interested in PARP-1 nucleolar substrates since the function of nucleolar PARP-1 is not clear. Three nucleolus proteins, YOR056C (NOB1), YMR290C (HAS1), and YDL051W (LHP1), were randomly chosen for further validation of poly(ADP-ribosyl)ation. These proteins were overexpressed in *E. coli* as His_6-tagged fusions and purified to near homogeneity (Figure 5A). The poly(ADP-ribosyl)ation of these proteins by PARP-1 was confirmed by activity blot assays and SDS−PAGE autoradiography using [^{32}P]NAD^+ as the PARP-1 assay substrates (Figure 5B,C). Yeast HAS1, a predicted RNA helicase, displayed much stronger poly(ADP-ribosyl)ation than the other two yeast proteins, and the automodification of PARP-1 decreased upon the addition of HAS1 (Figure 5C, lane 5).

Yeast Cells Expressing PARP-1 Have Lower Ribosome and Polysome Levels Than Control Cells. The nucleolus is responsible for rRNA transcription and ribosome biogenesis. Because PARP-1 is primarily localized in nucleoli and can modify some yeast nucleolar proteins *in vitro*, it is of interest to investigate whether yeast ribosome biogenesis is affected by PARP-1 expression. Accordingly, we compared the sucrose gradient profiles of ribosomal subunits and polyribosomes obtained from the pYES2 control cells and PARP-1-expressing cells. With no specific defect in the 40S or 60S subunits, the yeast PARP-1-expressing cells consistently display much lower abundance of 40S and 60S particles, 80S ribosome, and polysomes than the control cells (Figure 6). This result suggests that ribosome biogenesis is seriously affected by PARP-1 expression.

Human DDX 47 and La Proteins, the Homologues of Yeast HAS1 and LHP1, Are PARP-1 Substrates in Vitro. Although many human genes are not present in yeast, it has been predicted that 46% of identified human proteins have a yeast homologue (*23*). There is no endogenous PARP-1 in yeast, but some of the proteins involved in the human PARP-1 pathway may be conserved in yeast. Therefore, we investigated whether the human homologues of the yeast proteins identified in the yeast proteome microarray could also be modified by PARP-1. The human homologues of yeast proteins LHP1 and HAS1 were chosen for study. Human autoantigen La (SS-B) shares 25.9% sequence identity to yeast LHP1 and resembles LHP1 in both biochemical properties and cellular functionality (*24*). Yeast HAS1 is a member of the DEAD box family. It is highly related to human DEAD box protein DDX47 (37.7% identity). Neither human La nor DDX47 have been previously reported to be PARP-1 substrates. Recombinant human La and DDX47 proteins were overexpressed and purified from *E. coli*. The purified

Table 1: PARP-1 Substrates Identified by Yeast Proteome Microarray Screening[a]

ORF	common name	localization	protein class
YLR150W	STM1	nucleus	ribosomes and subtelomeric Y′ DNA binding protein
YDR432W	NPL3	nucleus	RNA binding protein that exports poly(A)$^+$ mRNA into the cytoplasm
YDR120C	TRM1	nucleus	tRNA methyltransferase
YOR198C	BFR1	nucleus	component of mRNP complexes associated with polyribosomes
YDR381W	YRA1	nucleus	protein required for export of poly(A)$^+$ mRNA from the nucleus
YPL133C	RDS2	nucleus	zinc cluster protein that has transcription regulator activity
YDL078C	MDH3	nucleus	malate dehydrogenase
YIL075C	RPN2	nucleus	subunit of the 26S proteasome
YDR257C	SET7	nucleus	protein that mediates methyltransferase activity in other proteins
YIL010W	DOT5	nucleus	protein involved in derepression of telomeric silencing
YMR153W	NUP53	nucleus	subunit of the nuclear pore complex
YNL186W	UBP10	nucleus	ubiquitin-specific protease
YMR039C	SUB1	nucleus	transcriptional coactivator
YOR288C	MPD1	nucleus	protein disulfide isomerase
YDL051W	LHP1	nucleus	RNA binding protein required for maturation of tRNA and snRNA
YLR003C	CMS1	nucleus	subunit of 90S preribosome processome complex
YER082C	UTP7	nucleolus	component of 40S subunit processosome that contains U3 snoRNA
YOR078W	BUD21	nucleolus	component of 40S subunit processosome that contains U3 snoRNA
YPL146C	NOP53	nucleolus	protein involved in biogenesis of the 60S subunit of the ribosome
YMR290C	HAS1	nucleolus	RNA helicase and constituent of 66S preribosomal particles
YOR056C	NOB1	nucleolus	protein involved in synthesis of 40S ribosomal subunits
YCR016W	N/A	nucleolus	unknown
YHL033C	RPL8A	cytoplasm	ribosomal protein L4 of the large ribosomal subunit
YBR031W	RPL4A	cytoplasm	component of the large ribosomal subunit
YBR118W	TEF2	cytoplasm	translational elongation factor EF-1α
YNL227C	JJJ1	cytoplasm	chaperone protein
YPR139C	VPS66	cytoplasm	protein involved in vacuolar protein sorting
YPR115W	GCA1	cytoplasm	protein predicted to function as a glycerol channel activator
YKL023W	N/A	cytoplasm	putative protein predicted to be involved in mRNA degradation
YBL055C	N/A	cytopalsm	3′−5′ exonuclease and endonuclease predicted to function in apoptosis
YBR222C	PCS60	peroxisome	peroxisomal AMP binding protein
YHR117W	TOM71	mitochondrion	mitochondrial outer membrane protein
YOR309C	N/A	N/A	unknown

[a]The cellular localization and functions of these proteins were taken from the SGD Web site (SGD project, "Saccharomyces Genome Database" http://www.yeastgenome.org/ (June 30, 2009)).

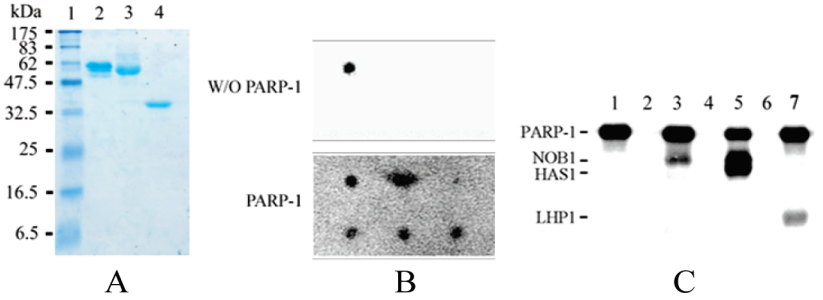

FIGURE 5: Purification and *in vitro* poly(ADP-ribosyl)ation of yeast proteins. (A) 12% SDS−PAGE gel analysis of the heterologously produced His_6-tagged yeast proteins. Lane 1, molecular mass markers; lane 2, NOB1; lane 3, HAS1; lane 4, LHP1. (B) Activity dot blot assay showing the poly(ADP-ribosyl)ation of yeast proteins by PARP-1. The spotting patterns on both upper (without PARP-1 reaction) and lower (with PARP-1 reaction) panels are the same. Top row (from left to right): PARP-1, histones, BSA. Bottom row: NOB1, HAS1, LHP1. (C) Poly(ADP-ribosyl)ation of yeast proteins by PARP-1 shown by SDS−PAGE autoradiography. Lanes 1, 3, 5, and 7 show the PARP-1 automodification and PARP-1 transmodification of the selected yeast proteins. Lane 1, PARP-1 only; lane 3, PARP-1 and NOB1; lane 5, PARP-1 and HAS1; lane 7, PARP-1 and LHP1. Lanes 2, 4, and 6 are negative controls without PARP-1 but are otherwise identical to lanes 3, 5, and 7, respectively.

human La and DDX47 were subjected to the *in vitro* poly(ADP-ribosyl)ation assay. The results clearly show that these two human proteins can be modified by PARP-1 *in vitro* (Figure 7).

DISCUSSION

In mammalian cells, PARP-1 controls cell proliferation through multiple mechanisms including regulation of cell cycle checkpoints, mitotic spindle formation, and centromere and centrosomal functions (*25*). Both the primary PARP-$1^{-/-}$ fibroblast and immortalized PARP-$1^{-/-}$ fibroblast display a G_2/M accumulation and multinuclear morphology (*6*, *26*). An appropriate expression level of PARP-1 also seems to be crucial, since overexpression of PARP-1 in NB4 acute promyelocytic leukemia cells promotes cell cycle arrest (*29*). The effect of PARP-1 expression on the yeast cell cycle (G_2/M delay) demonstrated in this study indicates that although PARP-1 is absent in yeast, it still retains its function as a negative regulator of cell proliferation

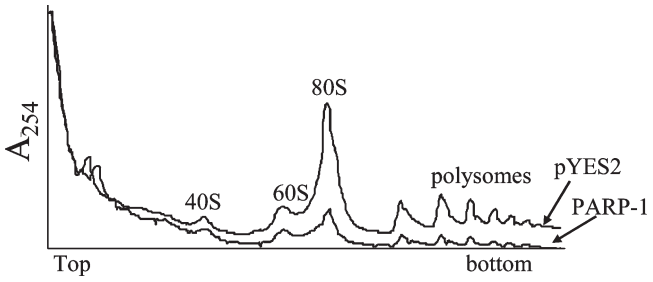

FIGURE 6: Analysis of the polysomal ribosome profile derived from pYES2 control cells and PARP-1-expressing cells. Positions of 40S and 60S ribosomal subunits, 80S ribosome, and polysomes are indicated.

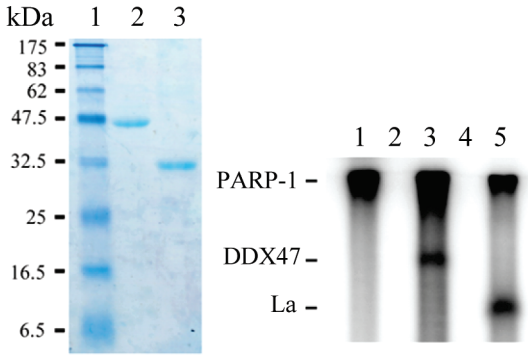

FIGURE 7: Purification and *in vitro* poly(ADP-ribosyl)ation of human proteins. (A) 12% SDS−PAGE gel analysis of the heterologously produced His_6-tagged human proteins. Lane 1, molecular mass markers; lane 2, human DDX47 protein; lane 3, human La protein. (B) Poly(ADP-ribosyl)ation of human DDX47 and La proteins by PARP-1 shown by SDS−PAGE autoradiography. The reaction mixtures loaded onto lanes 1, 3, and 5 contain PARP-1 alone (lane 1), with human DDX47 (lane 3), and with La protein (lane 5). The reaction mixtures loaded onto lanes 2 and 4 were identical to those loaded onto lanes 3 and 5, respectively, except PARP-1 was omitted from the assay mixture.

when heterologously expressed in yeast. However, it should be noted that PARP-1 overexpression has been found in early stage colon carcinogenesis (*27*), and PARP-1 can also enhance cell proliferation of colorectal cancer cells (*28*). These observations suggest that PARP-1 may in fact serve as both a positive and a negative regulator of cell cycle progression in mammalian cells.

PARP-1 is not evenly distributed within the yeast nucleus. No consensus sequence for a nucleolar localization signal has been established, but the localization of PARP-1 in the nucleolus has been demonstrated in several different mammalian cell types (*30*−*32*). Our results show that human PARP-1 also concentrates in the nucleolus when heterologously expressed in yeast, indicating that the mechanism for retaining PARP-1 in the nucleolus may be similar between mammalian and yeast cells. The accumulation of PARP-1 in the nucleolus might be the result of functional interactions with other nucleolar components (*30*−*32*). Previous studies have demonstrated that nucleolar localization of PARP-1 is dependent on active rRNA transcription (*30*). Consistent with the observation that PARP-1 binds to single-stranded DNA, RNA, and DNA−RNA duplexes, Desnoyers et al. proposed that the high-frequency transcription of rRNA in nucleoli provides many potential binding sites for PARP-1 that may lead to its nucleolar accumulation (*30*). Alternatively, PARP-1 may also bind to the protein components of the nucleolus. This is supported by the current study, where several nucleolus-associated proteins were identified as poly(ADP-ribosyl)ation substrates.

In mammalian cells, it is widely accepted that PARP-1 plays an active role in both nonspecific and gene-specific transcription regulation. PARP-1 regulates gene transcription by modulating chromatin structure, binding to sequence-specific gene promoters and acting as a component of enhancer/promoter regulatory complexes (*33*, *34*). Keeping this in mind, we also compared the mRNA levels between the PARP-1-expressing and control yeast cells by DNA microarray to determine if yeast growth inhibition could be attributed to a significant change in gene expression. However, results from clustering analysis showed similar gene expression patterns in both strains throughout the time course (our unpublished data). Thus, the effects of human PARP-1 on yeast gene transcription (if any) do not appear to be dramatic. It is generally believed that PARP-1 is activated by damaged DNA. However, recent studies indicate that PARP-1 can also be activated by nondamaged DNA. Interestingly, unlike mammalian cells, in which PARP-1's basal activity is very low, perhaps due to low enzyme activation, the heterologously expressed human PARP-1 in yeast is constitutively active under normal physiological conditions without DNA damage. This activity may mask the impact of PARP-1 on gene transcription.

The majority of the PARP-1 substrate proteins identified to date including those identified in this study are nuclear proteins with DNA or RNA binding abilities. Nucleic acids may act as mediators to bring PARP-1 and its substrate proteins together. PARP-1 substrates may also be anchored in the vicinity of PARP-1 by interacting with PAR, which is formed by PARP-1 automodification. While no consensus sequence for poly(ADP-ribosyl)ation has emerged, several poly(ADP-ribosyl)ation binding motifs have been identified in eukaryotic nuclear proteins (*35*−*38*). Consistent with our observation that PARP-1 is concentrated in the nucleoli of yeast cells, six yeast nucleolar proteins (UTP7, BUD21, NOB1, HAS1, NOP53, and LHP1) were identified as PARP-1 substrates in our high-throughput screen. Collectively, these proteins are involved in rRNA processing and ribosome biogenesis. UTP7 and BUD21 are components of the small subunit (SSU) processome, which is involved in processing pre-18S rRNA (*39*). NOB1 is required for cleavage of the 20S pre-rRNA to generate the mature 18S rRNA (*40*). HAS1 is required for the maturation of 18S rRNA, for the biogenesis of the 40S subunit, and for the processing of 27S pre-rRNAs during 60S subunit biogenesis (*41*, *42*). NOP53 is involved in the processing of 27S pre-rRNA and is important for the biogenesis of the 60S subunit (*43*). *NOP53* mutants cause significant growth defects and display significant 60S subunit deficiencies (*43*). LHP1 is required for maturation of tRNA and snRNA precursors (*44*, *45*). Among the identified cytosolic proteins, TEF2 is a translational elongation factor (*46*), and JJJ1 is required for a late step of 60S ribosomal subunit biogenesis (*47*), whereas RPL8A and RPL4A are both components of the large ribosomal subunit (*48*). Thus, it is conceivable that PARP-1 expression in yeast cells may exert some level of control over cellular processes by regulating protein synthesis. The polysome profiles confirm that the ribosome levels are significantly lower in the presence of PARP-1 expression. Poly(ADP-ribosyl)ation of nucleolar proteins may adversely affect ribosome biogenesis, perhaps by preventing proper rRNA maturation or by inhibiting the assembly of the functional ribosomes.

While proteome microarray provides an efficient and high-throughput screening method for identifying PARP-1 substrates,

some limitations associated with this analysis have to be noted. First, it cannot reproduce cellular localization effects; thus, some targets from microarray screening might not be modified in the cellular environment due to the localization restrictions. Second, some substrates may be part of complexes, which are difficult to recapitulate on a microarray. Third, whether proteins in an immobilized state can maintain the proper folding and function over a long period of storage still remains untested for proteome microarray. Therefore, caution should be taken to properly interpret the data from microarray screening, and additional experiments are needed to verify the screening results.

Since many basic biological processes in eukaryotes are well conserved, the yeast proteome screening could provide clues about PARP-1 substrates in multicellular organisms. Indeed, we were able to demonstrate that DDX47 and La (the human homologues of the yeast HAS1 and LHP1 proteins, respectively) were *in vitro* poly(ADP-ribosyl)ation substrates for PARP-1. In mammals, after DNA damage, it is of primary importance to stop replication at certain check points to allow for DNA repair. In addition to its established role in mediating DNA damage repair by recruitment of repair machinery to the sites of DNA damage, we propose that PARP-1 may also affect ribosome biogenesis in order to slow down cellular metabolism. In this scenario, when there is extensive DNA damage, overactivation of PARP-1 would not only deplete the cellular supply of NAD^+ but would also disrupt protein synthesis, slowing cellular metabolism and accelerating the process of cell necrosis. Preliminary results using a human proteome microarray show that most of the human homologues of the yeast PARP-1 substrates can also be modified by PARP-1, once again supporting the idea that there are functional similarities between PARP-1 activity in both humans and yeast. Whether these proteins are indeed PARP-1 physiological substrates and whether their cellular functions are changed upon poly(ADP-ribosyl)ation require further investigation.

In summary, although PARP-1 is absent in yeast, it still concentrates in the nucleolus and retains its function as a negative regulator of cell proliferation when heterologously expressed in yeast. PARP-1 expression in yeast cells may exert some level of control over cellular processes by regulating protein synthesis, and the polysome profiles confirm that the yeast ribosome levels are significantly lower in the presence of PARP-1 expression. These results suggest that there are certain functional similarities between PARP-1 activity in both humans and yeast. However, unlike the mammalian cells, in which PARP-1 is activated by damaged DNA, the expressed human PARP-1 in yeast is active under normal physiological conditions without DNA damage. While this constitutive activity could mask the impact of PARP-1 on gene transcription, it may be useful for direct probing the biological consequence of poly(ADP-ribosyl)ation of proteins and screening of chemical libraries for PARP inhibitors. Further investigation of the biological relevance in mammalian cells of poly(ADP-ribosyl)ation of nucleolar proteins found in this study is in progress.

ACKNOWLEDGMENT

The authors thank Professor Vishwanath Iyer (The University of Texas at Austin) for help on the DNA microarray experiments and for useful discussions, Professor Arlen W. Johnson (The University of Texas at Austin) for the plasmid pAJ1076, Professor Michael Snyder (Yale University) for the cDNAs encoding yeast NOB1, HAS1, and LHP1, Madhavi Challa (The University of Texas at Austin) for help with flow cytometry, Angela Bardo from the Microscopy and Imaging Facility (Institute for Cellular and Molecular Biology at The University of Texas at Austin) for help with fluorescence microscopy, Nai-Jung Hung (The University of Texas at Austin) for help with polysome profile analysis, and Christopher Thibodeaux and Dr. Mark Ruszczycky for comments of the manuscript.

REFERENCES

1. D'Amours, D., Desnoyers, S., D'Silva, I., and Poirier, G. G. (1999) Poly(ADP-ribosyl)ation reactions in the regulation of nuclear functions. *Biochem. J. 342* (Part 2), 249–268.
2. Kim, M. Y., Zhang, T., and Kraus, W. L. (2005) Poly(ADP-ribosyl)-ation by PARP-1: "PAR-laying" NAD^+ into a nuclear signal. *Genes Dev. 19*, 1951–1967.
3. Meyer-Ficca, M. L., Meyer, R. G., Jacobson, E. L., and Jacobson, M. K. (2005) Poly(ADP-ribose) polymerases: managing genome stability. *Int. J. Biochem. Cell Biol. 37*, 920–926.
4. Tulin, A., and Spradling, A. (2003) Chromatin loosening by poly-(ADP)-ribose polymerase (PARP) at *Drosophila puff* loci. *Science 299*, 560–562.
5. Kim, M. Y., Mauro, S., Gevry, N., Lis, J. T., and Kraus, W. L. (2004) NAD^+-dependent modulation of chromatin structure and transcription by nucleosome binding properties of PARP-1. *Cell 119*, 803–814.
6. de Murcia, J. M., Niedergang, C., Trucco, C., Ricoul, M., Dutrillaux, B., Mark, M., Oliver, F. J., Masson, M., Dierich, A., and LeMeur, M.; et al. (1997) Requirement of poly(ADP-ribose) polymerase in recovery from DNA damage in mice and in cells. *Proc. Natl. Acad. Sci. U.S.A. 94*, 7303–7307.
7. Wang, Z. Q., Auer, B., Stingl, L., Berghammer, H., Haidacher, D., Schweiger, M., and Wagner, E. F. (1995) Mice lacking ADPRT and poly(ADP-ribosyl)ation develop normally but are susceptible to skin disease. *Genes Dev. 9*, 509–520.
8. Molinete, M., Vermeulen, W., Burkle, A., Menissier-de Murcia, J., Kupper, J. H., Hoeijmakers, J. H., and de Murcia, G. (1993) Overproduction of the poly(ADP-ribose) polymerase DNA-binding domain blocks alkylation-induced DNA repair synthesis in mammalian cells. *EMBO J. 12*, 2109–2117.
9. Ding, R., Pommier, Y., Kang, V. H., and Smulson, M. (1992) Depletion of poly(ADP-ribose) polymerase by antisense RNA expression results in a delay in DNA strand break rejoining. *J. Biol. Chem. 267*, 12804–12812.
10. Cepeda, V., Fuertes, M. A., Castilla, J., Alonso, C., Quevedo, C., Soto, M., and Perez, J. M. (2006) Poly(ADP-ribose) polymerase-1 (PARP-1) inhibitors in cancer chemotherapy. *Recent Patents Anticancer Drug Discov. 1*, 39–53.
11. Otto, H., Reche, P. A., Bazan, F., Dittmar, K., Haag, F., and Koch-Nolte, F. (2005) In silico characterization of the family of PARP-like poly(ADP-ribosyl)transferases (pARTs). *BMC Genomics 6*, 139.
12. Menissier de Murcia, J., Ricoul, M., Tartier, L., Niedergang, C., Huber, A., Dantzer, F., Schreiber, V., Ame, J. C., Dierich, A., and LeMeur, M.; et al. (2003) Functional interaction between PARP-1 and PARP-2 in chromosome stability and embryonic development in mouse. *EMBO J. 22*, 2255–2263.
13. Sbodio, J. I., and Chi, N. W. (2002) Identification of a tankyrase-binding motif shared by IRAP, TAB182, and human TRF1 but not mouse TRF1. NuMA contains this RXXPDG motif and is a novel tankyrase partner. *J. Biol. Chem. 277*, 31887–31892.
14. Schreiber, V., Ame, J. C., Dolle, P., Schultz, I., Rinaldi, B., Fraulob, V., Menissier-de Murcia, J., and de Murcia, G. (2002) Poly(ADP-ribose) polymerase-2 (PARP-2) is required for efficient base excision DNA repair in association with PARP-1 and XRCC1. *J. Biol. Chem. 277*, 23028–23036.
15. Kaiser, P., Auer, B., and Schweiger, M. (1992) Inhibition of cell proliferation in *Saccharomyces cerevisiae by* expression of human NAD^+ ADP-ribosyltransferase requires the DNA binding domain ("zinc fingers"). *Mol. Gen. Genet. 232*, 231–239.
16. Avila, M. A., Velasco, J. A., Smulson, M. E., Dritschilo, A., Castro, R., and Notario, V. (1994) Functional expression of human poly-(ADP-ribose) polymerase in *Schizosaccharomyces pombe* results in mitotic delay at G1, increased mutation rate, and sensitization to radiation. *Yeast 10*, 1003–1017.
17. Collinge, M. A., and Althaus, F. R. (1994) Expression of human poly(ADP-ribose) polymerase in *Saccharomyces cerevisiae*. *Mol. Gen. Genet. 245*, 686–693.

18. Perkins, E., Sun, D., Nguyen, A., Tulac, S., Francesco, M., Tavana, H., Nguyen, H., Tugendreich, S., Barthmaier, P., and Couto, J.; et al. (2001) Novel inhibitors of poly(ADP-ribose) polymerase/PARP1 and PARP2 identified using a cell-based screen in yeast. *Cancer Res. 61*, 4175–4183.
19. Greenhalf, W., Lee, J., and Chaudhuri, B. (1999) A selection system for human apoptosis inhibitors using yeast. *Yeast 15*, 1307–1321.
20. Geiser, M., Cebe, R., Drewello, D., and Schmitz, R. (2001) Integration of PCR fragments at any specific site within cloning vectors without the use of restriction enzymes and DNA ligase. *BioTechniques 31*, 88–92.
21. Zhang, J., and Snyder, S. H. (1993) Purification of a nitric oxide-stimulate ADP-ribosylated protein using biotinylated β-nicotinamide adenine dinucleotide. *Biochemistry 32*, 2228–2233.
22. West, M., Hedges, J. B., Chen, A., and Johnson, A. W. (2005) Defining the order in which Nmd3p and Rpl10p load onto nascent 60S ribosomal subunits. *Mol. Cell. Biol. 25*, 3802–3813.
23. Lander, E. S., Linton, L. M., Birren, B., Nusbaum, C., Zody, M. C., Baldwin, J., Devon, K., Dewar, K., Doyle, M., and FitzHugh, W.; et al. (2001) Initial sequencing and analysis of the human genome. *Nature 409*, 860–921.
24. Yoo, C. J., and Wolin, S. L. (1994) La proteins from *Drosophila melanogaster* and *Saccharomyces cerevisiae*: a yeast homolog of the La autoantigen is dispensable for growth. *Mol. Cell. Biol. 14*, 5412–5424.
25. Schreiber, V., Dantzer, F., Ame, J. C., and de Murcia, G. (2006) Poly(ADP-ribose): novel functions for an old molecule. *Nat. Rev. Mol. Cell. Biol. 7*, 517–528.
26. Trucco, C., Oliver, F. J., de Murcia, G., and Menissier-de Murcia, J. (1998) DNA repair defect in poly(ADP-ribose) polymerase-deficient cell lines. *Nucleic Acids Res. 26*, 2644–2649.
27. Nosho, K., Yamamoto, H., Mikami, M., Taniguchi, H., Takahashi, T., Adachi, Y., Imamura, A., Imai, K., and Shinomura, Y. (2006) Overexpression of poly(ADP-ribose) polymerase-1 (PARP-1) in the early stage of colorectal carcinogenesis. *Eur. J. Cancer 42*, 2374–2381.
28. Idogawa, M., Yamada, T., Honda, K., Sato, S., Imai, K., and Hirohashi, S. (2005) Poly(ADP-ribose) polymerase-1 is a component of the oncogenic T-cell factor-4/beta-catenin complex. *Gastroenterology 128*, 1919–1936.
29. Bhatia, M., Kirkland, J. B., and Meckling-Gill, K. A. (1996) Over-expression of poly(ADP-ribose) polymerase promotes cell cycle arrest and inhibits neutrophilic differentiation of NB4 acute promyelocytic leukemia cells. *Cell Growth Differ. 7*, 91–100.
30. Desnoyers, S., Kaufmann, S. H., and Poirier, G. G. (1996) Alteration of the nucleolar localization of poly(ADP-ribose) polymerase upon treatment with transcription inhibitors. *Exp. Cell. Res. 227*, 146–153.
31. Meder, V. S., Boeglin, M., de Murcia, G., and Schreiber, V. (2005) PARP-1 and PARP-2 interact with nucleophosmin/B23 and accumulate in transcriptionally active nucleoli. *J. Cell Sci. 118*, 211–222.
32. Mosgoeller, W., Steiner, M., Hozak, P., Penner, E., and Wesierska-Gadek, J. (1996) Nuclear architecture and ultrastructural distribution of poly(ADP-ribosyl)transferase, a multifunctional enzyme. *J. Cell Sci. 109* (Part 2), 409–418.
33. Butler, A. J., and Ordahl, C. P. (1999) Poly(ADP-ribose) polymerase binds with transcription enhancer factor 1 to MCAT1 elements to regulate muscle-specific transcription. *Mol. Cell. Biol. 19*, 296–306.
34. Kraus, W. L., and Lis, J. T. (2003) PARP goes transcription. *Cell 113*, 677–683.
35. Pleschke, J. M., Kleczkowska, H. E., Strohm, M., and Althaus, F. R. (2000) Poly(ADP-ribose) binds to specific domains in DNA damage checkpoint proteins. *J. Biol. Chem. 275*, 40974–40980.
36. Gagne, J. P., Hunter, J. M., Labrecque, B., Chabot, B., and Poirier, G. G. (2003) A proteomic approach to the identification of heterogeneous nuclear ribonucleoproteins as a new family of poly(ADP-ribose)-binding proteins. *Biochem. J. 371*, 331–340.
37. Ahel, I., Ahel, D., Matsusaka, T., Clark, A. J., Pines, J., Boulton, S. J., and West, S. C. (2008) Poly(ADP-ribose)-binding zinc finger motifs in DNA repair/checkpoint proteins. *Nature 451*, 81–85.
38. Karras, G. I., Kustatscher, G., Buhecha, H. R., Allen, M. D., Pugieux, C., Sait, F., Bycroft, M., and Ladurner, A. G. (2005) The macro domain is an ADP-ribose binding module. *EMBO J. 24*, 1911–1920.
39. Dragon, F., Gallagher, J. E., Compagnone-Post, P. A., Mitchell, B. M., Porwancher, K. A., Wehner, K. A., Wormsley, S., Settlage, R. E., Shabanowitz, J., and Osheim, Y.; et al. (2002) A large nucleolar U3 ribonucleoprotein required for 18S ribosomal RNA biogenesis. *Nature 417*, 967–970.
40. Fatica, A., Oeffinger, M., Dlakic, M., and Tollervey, D. (2003) Nob1p is required for cleavage of the 3′ end of 18S rRNA. *Mol. Cell. Biol. 23*, 1798–1807.
41. Rocak, S., Emery, B., Tanner, N. K., and Linder, P. (2005) Characterization of the ATPase and unwinding activities of the yeast DEAD-box protein Has1p and the analysis of the roles of the conserved motifs. *Nucleic Acids Res. 33*, 999–1009.
42. Emery, B., de la Cruz, J., Rocak, S., Deloche, O., and Linder, P. (2004) Has1p, a member of the DEAD-box family, is required for 40S ribosomal subunit biogenesis in *Saccharomyces cerevisiae*. *Mol. Microbiol. 52*, 141–158.
43. Sydorskyy, Y., Dilworth, D. J., Halloran, B., Yi, E. C., Makhnevych, T., Wozniak, R. W., and Aitchison, J. D. (2005) Nop53p is a novel nucleolar 60S ribosomal subunit biogenesis protein. *Biochem. J. 388*, 819–826.
44. Pannone, B. K., Xue, D., and Wolin, S. L. (1998) A role for the yeast La protein in U6 snRNP assembly: evidence that the La protein is a molecular chaperone for RNA polymerase III transcripts. *EMBO J. 17*, 7442–7453.
45. Yoo, C. J., and Wolin, S. L. (1997) The yeast La protein is required for the 3′ endonucleolytic cleavage that matures tRNA precursors. *Cell 89*, 393–402.
46. Schirmaier, F., and Philippsen, P. (1984) Identification of two genes coding for the translation elongation factor EF-1 alpha of *S. cerevisiae*. *EMBO J. 3*, 3311–3315.
47. Meyer, A. E., Hung, N. J., Yang, P., Johnson, A. W., and Craig, E. A. (2007) The specialized cytosolic J-protein, Jjj1, functions in 60S ribosomal subunit biogenesis. *Proc. Natl. Acad. Sci. U.S.A. 104*, 1558–1563.
48. Planta, R. J., and Mager, W. H. (1998) The list of cytoplasmic ribosomal proteins of *Saccharomyces cerevisiae*. *Yeast 14*, 471–477.